A probability assessment of encountering dayside magnetopause diffusion regions

S. T. Griffiths,[1] S. M. Petrinec,[2] K. J. Trattner,[2] S. A. Fuselier,[2] J. L. Burch,[3] T. D. Phan,[4] and V. Angelopoulos[5]

Received 28 January 2010; revised 3 October 2010; accepted 7 October 2010; published 18 February 2011.

[1] Probability maps for encountering the reconnection electron diffusion region of the dayside magnetopause have been developed using a model of reconnection and solar wind observations. The maps indicate that along the magnetopause surface, the chance of directly sampling the diffusion region during a given season varies considerably. The probability distribution depends strongly on the distribution of interplanetary magnetic field directions and, also, is significantly influenced by the Earth's intrinsic magnetic dipole field tilt angle. The probability also scales with the assumed size of the diffusion region. The probability distribution shows little dependence on the phase of the solar cycle.

Citation: Griffiths, S. T., S. M. Petrinec, K. J. Trattner, S. A. Fuselier, J. L. Burch, T. D. Phan, and V. Angelopoulos (2011), A probability assessment of encountering dayside magnetopause diffusion regions, *J. Geophys. Res.*, *116*, A02214, doi:10.1029/2010JA015316.

1. Introduction

[2] Magnetic reconnection has been established as the primary mechanism by which shocked solar wind plasma is transported across the magnetopause and into the magnetosphere. Although there have been many observations of reconnection signatures in the reconnection outflow region at the Earth's magnetopause [e.g., *Paschmann et al.*, 1979; *Sonnerup et al.*, 1981; *Gosling et al*., 1986], direct sampling of the reconnection diffusion region itself is difficult and rare [cf. *Mozer et al.*, 2002; *Scudder et al*., 2002; *Mozer et al*., 2008]. The rarity of encounters is due to the very large sampling space in relation to the inherent scales of the physical process. The fundamental physics of reconnection occurs within diffusion layers (ion and electron), wherein the "frozen-in" conditions of the collisionless plasma break down, allowing plasmas (and associated magnetic fields) in different regimes to interact and topologically reconfigure. The magnetopause diffusion regions are believed to be of the order of 1 to 10 km thick and ~100 km [*Hesse et al*., 1999; *Drake et al*., 2003] or more [*Pritchett and Mozer*, 2009] long. On the basis of various remote observations, dayside magnetopause reconnection is not believed to occur often at isolated, patchy locations. Rather, owing to the gradual variation in fields and particle populations along the magnetopause surface, magnetic reconnection is believed to occur along an x line, extending tens of Earth radii along the dayside magnetopause [*Phan et al.*, 2000, 2006]. Thus, magnetopause reconnection is thought to often occur along thin, ribbon-like regions: very long along the magnetopause surface, but limited in spatial thickness (i.e., length of the diffusion region) and width. Since sampling spacecraft are obviously resource limited, it is important to estimate the most probable locations for magnetic reconnection and optimize mission parameters to encounter those regions. This is especially important for the upcoming Magnetospheric Multiscale (MMS) mission.

[3] In this study, maps of reconnection probability at the dayside magnetopause are developed for various extended time intervals. Several months of solar wind observations are used, along with a phenomenological model of the location of magnetopause reconnection x lines (developed from remote sensing techniques).

2. Observations and Models

[4] Solar wind observations from the Advanced Composition Explorer (ACE) spacecraft at the L1 Lagrange point are used as magnetosphere model inputs. These include the interplanetary magnetic field (IMF) [*Smith et al.*, 1998] and solar wind density and velocity moments [*McComas et al.*, 1998]. The observations used span mid-2001 (near the solar maximum) to the end of 2006 (near solar minimum), at a 3 minute resolution.

[5] The magnetospheric magnetic field was simulated using the Tsyganenko 1996 semiempirical model (hereafter called the T96 model [*Tsyganenko*, 1995]). The T96 model confines the Earth's dayside magnetic field within a boundary representing the magnetopause, scaled by the solar wind dynamic pressure. The T96 model normally diffuses the IMF Y_{GSM} and Z_{GSM} components through the

[1]Department of Physics and Astronomy, University of Iowa, Iowa City, Iowa, USA.
[2]Lockheed Martin Advanced Technology Center, Palo Alto, California, USA.
[3]Southwest Research Institute, San Antonio, Texas, USA.
[4]Space Sciences Laboratory, University of California, Berkeley, California, USA.
[5]Institute of Geophysics and Planetary Physics, University of California, Los Angeles, California, USA.

Copyright 2011 by the American Geophysical Union.
0148-0227/11/2010JA015316

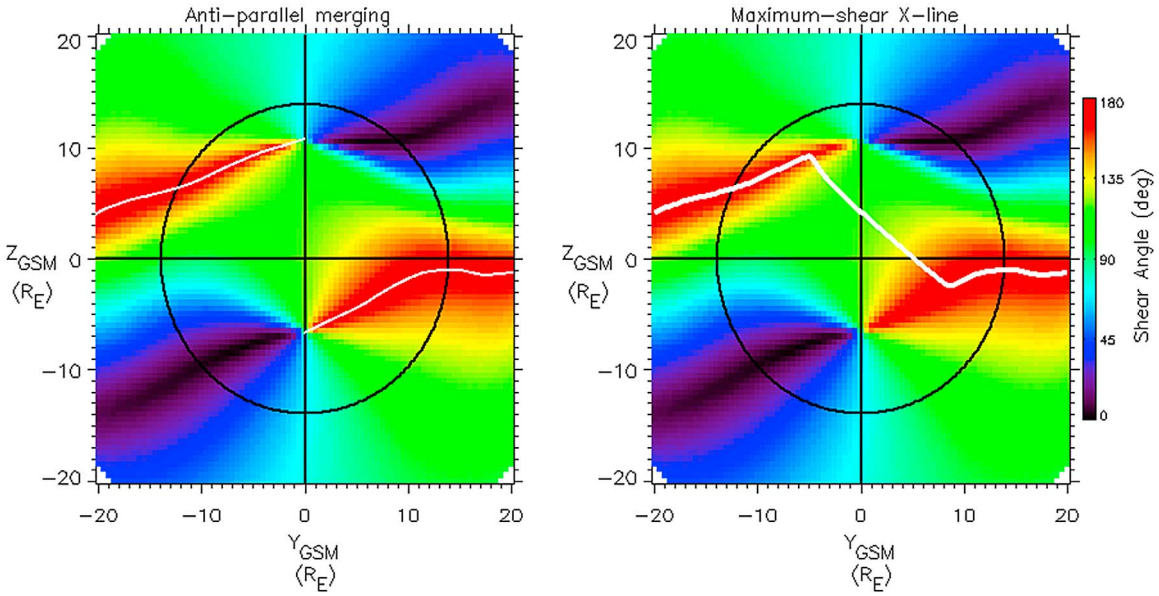

Figure 1. Magnetic shear angle plots with reconnection lines (white) overlain. (left) Antiparallel reconnection line. (right) Maximum shear x line used in the maximum magnetic shear model. The black circle represents the terminator plane.

magnetopause boundary. However, for this study no such diffusion of fields is allowed, so that possible reconnection locations can be located without any a priori model assumptions. For the given magnetopause size and shape, the IMF is draped across the magnetopause using the *Cooling et al.* [2001] model, and the magnetic shear angle (the angle between the draped IMF and the magnetospheric magnetic field at the magnetopause) is computed over the entire magnetopause surface.

[6] Several recent attempts have been made to determine the location of the x line at the dayside magnetopause. Theoretical models include those of *Lau and Finn* [1990] and *Wang and Bhattacharjee* [1996]. *Moore et al.* [2002] used semiempirical and analytic models to estimate the x line configuration along the dayside magnetopause. Numerical models of the location of the x line and its dependence on the IMF include those *Park et al.* [2006] and *Hu et al.* [2009]. *Pu et al.* [2007] used accelerated flow observations from DoubleStar and Cluster to estimate where the x line lies for the southward or dawnward IMF, while *Dunlop et al.* [2009] used observations from these spacecraft to document an occurrence of high-latitude (i.e., antiparallel) reconnection. A recent magnetic merging model proposed by *Trattner et al.* [2007] (hereafter referred to as the maximum magnetic shear model) also combines both antiparallel and component reconnection models and is based on observational evidence. This model was developed by analyzing more than 3000 distribution functions from 130 polar cusp crossings, using the low-velocity ion cutoff method of *Onsager et al.* [1990] on ion distribution functions as measured by the Toroidal Imaging Mass-Angle Spectrograph (TIMAS) instrument. Depending on the IMF conditions, this empirical model predicts that the reconnection x line position is given by either the antiparallel model or a combination of the antiparallel and the component x line, which is denoted as a maximum magnetic shear x line. Specifically, when the IMF clock angle is within 30° of 180° (clock angle = atan(IMF B_y/IMF B_z)) or when the IMF $B_{x\text{-GSM}}$ is large (>70% of the IMF magnitude), the maximum magnetic shear model predicts antiparallel reconnection. In all other cases the maximum magnetic shear model predicts that reconnection occurs along a maximum shear x line, which is mostly antiparallel except near the subsolar region, where a continuous and tilted x line connects to the bifurcated antiparallel regions. Northward IMF conditions are not considered in the maximum magnetic shear model, since the northward IMF is assumed generally to result in steady reconnection poleward of the cusps (though some studies have presented observational evidence that transitory reconnection may occur equatorward of the cusps [e.g., *Chandler et al.*, 1999; *Fuselier et al.*, 2000]). In this study northward IMF conditions are included only insofar as to reduce the overall probability of reconnection equatorward of the cusps.

[7] In practice the reconnection lines are computed from the magnetic shear angles. Antiparallel reconnection lines are computed first by finding the Z_{GSM} location of the maximum shears at ±20 R_E (Earth radii) along the Y_{GSM} axis. Once maximum shears are found at the left and right boundaries, one walks along the path of maximum shear toward the noon meridian (Y_{GSM} = 0). Computing the maximum magnetic shear model maximum shear x line requires that the antiparallel reconnection x line be computed first. The largest magnetic shear angle at low latitudes and at local noon is then determined (i.e., the ridge of the shear angle "saddle," corresponding to a surrogate subsolar point for the tilted x line), after which one walks away from local noon along a line of maximum shear until the two antiparallel lines are intersected. An example is shown in Figure 1.

[8] Because of the nature of the analytic models, a rigorous error analysis is not performed. It is expected that neither the

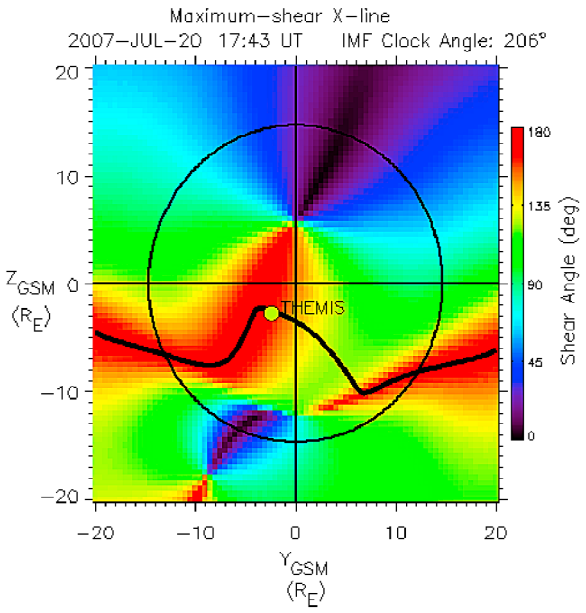

Figure 2. THEMIS C location (chartreuse-yellow marker) at the time of a magnetopause crossing through an ion diffusion region, as analyzed by *Mozer et al.* [2008]. The bold black line denotes the location of the maximum shear magnetopause x line, for the matched ACE solar wind conditions.

magnetosheath magnetic field model nor the T96 model perfectly represents the actual conditions. For example, the magnetosheath model of *Kobel and Flückiger* [1994] (on which the Cooling et al. model is based) does not satisfy the Rankine-Hugoniot conditions (i.e., the tangential magnetic field) across the bow shock, and this weakness is believed to be manifest in some manner as the field is draped around the model magnetopause. The T96 model is semiempirical but may not be especially accurate in regions where there is sparse data coverage. In addition, neither of these models captures all the dynamics of the system. This study thus adopts an uncertainty of ~1 R_E [see *Trattner et al.*, 2007] for the x line location calculation. It is noted that for large IMF B_x, the errors may be larger.

[9] As an example to illustrate the predictive capability of the maximum shear x line model, a direct comparison is presented of the model and observations for a Time History of Events and Macroscale Interactions during Substorms (THEMIS) crossing of the magnetopause [*Mozer et al.*, 2008]. A more complete study using the in situ observations from an entire spacecraft mission is beyond the scope of this study but is the subject of works in progress. Here the magnetopause crossing of 1743:30 UT, 20 July 2007, by THEMIS C is shown in Figure 2. This event has already been shown by *Mozer et al.* [2008] to be a crossing through an ion diffusion region. Figure 2 illustrates the magnetic shear angles across the magnetopause (as viewed from the Sun) for this time period. The corresponding solar wind parameters for this interval are as follows: B_x, +4.6 nT; B_y, −1.9 nT; B_z, −4.0 nT; v, 426 km/s; and n_i, 6.4 cm^{-3} (from ACE, convected by 53 min, 45 s, determined from convection speed, and refined by matching of magnetic field clock angles). Overlain in Figure 2 is the maximum shear x line for a steady IMF clock angle of 206° (solid black line) and the location of the THEMIS C spacecraft as it crossed the magnetopause. The location of the spacecraft is displaced from the antiparallel merging sites and, also, is farther southward of the equator than can be explained by a straight component x line passing through the subsolar location. However, the THEMIS C location at the magnetopause crossing matches very well the maximum shear x line for this case.

3. Analysis and Results

[10] Reconnection x lines along the dayside magnetopause and with a length of 1 R_E have been calculated at the 3 min solar wind data resolution using the maximum magnetic shear model described, spanning 6 years, from 2001 to 2006. The determined reconnection lines were then summed over a prescribed time interval (monthly and/or seasonal time periods) and divided by the total number of ACE solar wind intervals to produce a probability map of where magnetopause reconnection is most likely to occur. Specific months and seasons were selected as time divisions, grouped accordingly: spring (February–April), summer (May–July), fall (August–October), and winter (November–January).

[11] The ion and electron diffusion regions are believed to be long and thin. It is assumed in this study that the model x line is stable (i.e., continuously active but in a fixed configuration) during constant solar wind conditions, that it extends all the way to the flank regions, and that there is only a single x line (i.e., no flux ropes or O lines). Recent theoretical and observational work suggests that the electron outer diffusion region may be much more elongated than previously thought [*Daughton et al.*, 2006; *Karimabadi et al.*, 2007; *Phan et al.*, 2007; *Shay et al.*, 2007]: extending over tens of ion inertial lengths (d_i). Also, as determined from detailed simulations by *Pritchett and Mozer* [2009], especially in the case of asymmetric reconnection (as at the magnetopause) and in the presence of a guide field, the violation of the frozen-in condition for the electrons occurs in an elongated region of at least 10 d_i, or more than ≈1000 km. The corresponding region for ions is expected to be considerably larger. However, it should be noted that these studies pertain more appropriately to open systems, rather than one for which one end of a field line is anchored to the ionosphere.

[12] Since it is not understood how long the diffusion regions truly are (hence, the need for missions such as MMS), in this study a length of 1 R_E is ascribed to the diffusion region (which likely represents an extreme upper limit). The change in (i.e., scaling of) the probability maps for shorter diffusion-region lengths is discussed in the next section.

[13] Before proceeding, it must be pointed out that the probability maps produced from the 3 min resolution solar wind observations are independent of any spacecraft mission. Although a relatively short solar wind time resolution is used, the IMF clock angle can vary by several degrees within a given interval. In addition, the motion of a sampling spacecraft is usually slow relative to the motion of an oscillatory magnetopause boundary [cf. *Song et al.*, 1988], so that multiple crossings and partial crossings can occur within a single 3 min interval. There is thus the opportunity

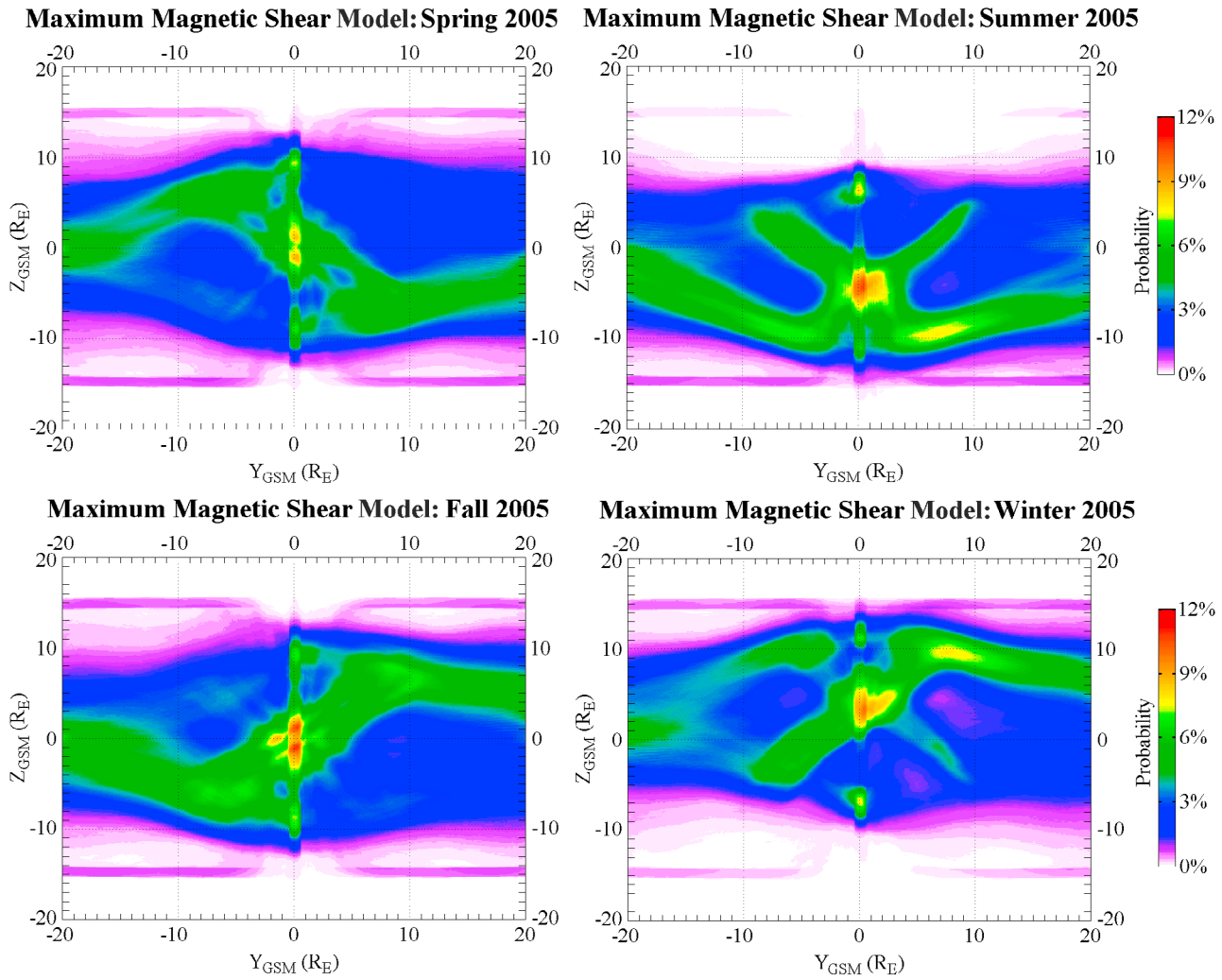

Figure 3. Maximum magnetic shear model seasonal reconnection x line location probability distributions for 2005.(top left) Spring, (top right) summer, (bottom left) fall, and (bottom right) winter.

for multiple chances of encountering the diffusion region during a given pass.

3.1. Seasonal Variations

[14] Clearly observable seasonal variations of the reconnection x line distribution due to the Earth's dipole tilt with respect to the Sun are expected, using the maximum magnetic shear model. Figure 3 shows the four seasons of year 2005, confirming the expectation of a strong seasonal dependence on the probability distributions. The spring and fall seasons are strongly biased in opposite senses according to the IMF B_y. This is a consequence of the Russell-McPherron effect [*Russell and McPherron*, 1973]. For a given season the probability of a diffusion-region encounter along the magnetopause surface ranges from near 0 up to ~5% on the flanks (assuming a diffusion-region length of 1 R_E). Along localized regions of the noon meridian the probability can be somewhat higher (due to overlap of positive and negative IMF B_y intervals). Similar behavior is observed for other years, with consistent trends.

[15] Perhaps the most important feature is the shifting high-probability region near the subsolar point. According to some traditional southward IMF component reconnection models (i.e., tilted neutral-line models described by *Sonnerup* [1974], *Cowley* [1976], and *Fuselier et al.* [2002]), reconnection should occur at the first point of contact of the solar wind with the magnetosphere (i.e., the subsolar point). However, the results of this study show this not to be the case. During the spring and fall there is indeed a high-probability reconnection region near the subsolar point, in good agreement with traditional component reconnection models. However, during the northern summer and winter seasons the higher probability region shifts south or north of the equator, respectively. The consequence of this seasonal effect is that a spacecraft near the subsolar point may encounter x line diffusion regions less frequently than expected.

[16] A high probability of reconnection can also appear frequently near the polar cusps. The polar cusps are at $Y_{GSM} = 0$ R_E and $Z_{GSM} \approx \pm 10$ R_E in Figure 3. This high probability is a consequence of the maximum magnetic shear model reverting to the antiparallel model for a large IMF B_x or when 150° < IMF clock angle < 210°. The near-cusp high-probability regions also shift according to season

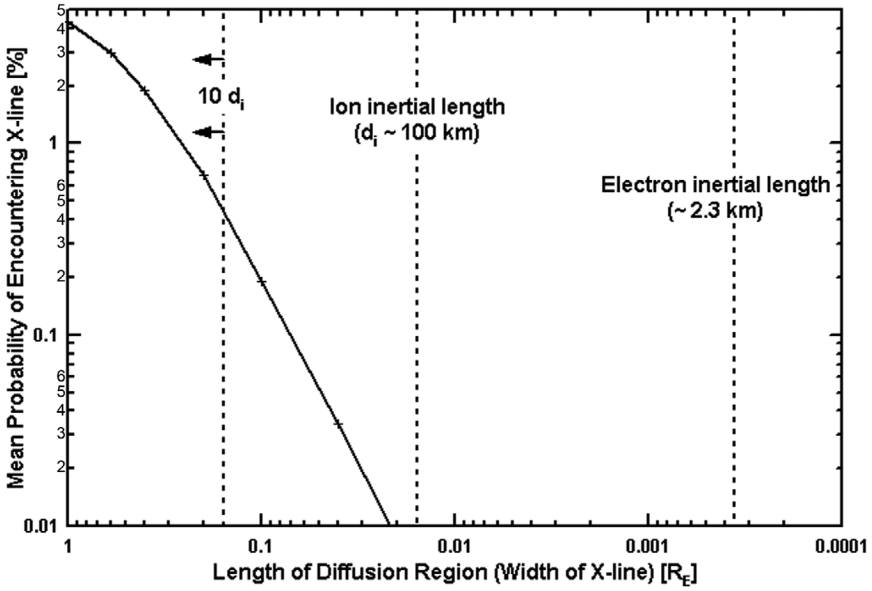

Figure 4. Scaling of the probability as a function of the length of the diffusion region (based on mean probabilities during the winter season). This study uses a length of 1 R_E for probability maps. However, the exact value (for either the ion or the electron diffusion region) is unknown and is a goal of the MMS mission.

in the same manner as the high-probability region near the subsolar point.

[17] Finally, relatively high probabilities are seen to the east and west of the subsolar point. A purely antiparallel model would predict a relatively low probability of observing a reconnection site in these locations. Instead, the antiparallel model predicts that reconnection occurs predominantly along lines that begin at the left and right boundaries and end at the polar cusps, leading to discontiguous x lines (Figure 1, left). The inclusion of the maximum shear x line in the maximum magnetic shear model causes features typical of both antiparallel and component reconnection models to appear. An important consequence is that a spacecraft following a highly elliptical orbit in the ecliptic plane should have a much higher probability of crossing the magnetopause near a reconnection site than predicted by the antiparallel model.

[18] In summary, there is a considerable seasonal effect on the probability distributions for encountering the reconnection diffusion regions. The dipole tilt angle is the cause of this variation.

[19] Figure 4 illustrates how the probabilities in the maps would scale with the length of the diffusion region, when encountering a completely static x line. For example, if the length of the electron diffusion region were only 10 d_i (the estimated minimum length within which electrons violate the frozen-in condition, as determined by the *Pritchett and Mozer* [2009] simulations), then all probabilities would be reduced by a factor of ~10.

3.2. Solar Cycle Variations

[20] It is of interest to understand whether the probability maps vary significantly on time scales of years. There are significant differences in the Sun's magnetic field at solar minimum versus at solar maximum. Near solar minimum the Sun's magnetic field grossly resembles a dipole with some quadrupole components and is oriented close to orthogonal to the ecliptic plane. At solar maximum local magnetic fields near sunspot regions contribute significantly to the Sun's total magnetic field, causing the IMF to exhibit more chaotic behavior. The average IMF conditions are also known to vary over the course of a solar cycle. Specifically, the standard deviation of IMF intensity (and components) was found to lower near the solar minimum than during other phases of the solar cycle [*Luhmann et al.*, 1993]. If systematic variations with solar cycle phase also occur in the IMF clock angle, then this may be reflected in the probability maps. The 6 year solar wind data set used here provides enough data to investigate a half solar cycle, from solar maximum to near solar minimum.

[21] Probability maps from the fall season at solar minimum and maximum are shown in Figure 5. The results show very little evidence that the reconnection x line probability distributions change significantly owing to solar cycle influences. While there are minor differences in the probability distributions between solar maximum and solar minimum, the general characteristics remain the same. The lack of major variations due to mechanisms that operate on the time scale of years is consistent throughout the results, both when comparing seasons and when comparing individual months. A possible explanation for the lack of yearly variations given the established impact of the solar cycle on solar wind conditions is that while the IMF intensity and component distributions vary between solar maximum and solar minimum, the distribution of IMF clock angles remains unchanged. Thus, the variations in the probability maps are primarily due to seasonal effects (i.e., the dipole tilt angle and the Russell-McPherron effect). Striations in

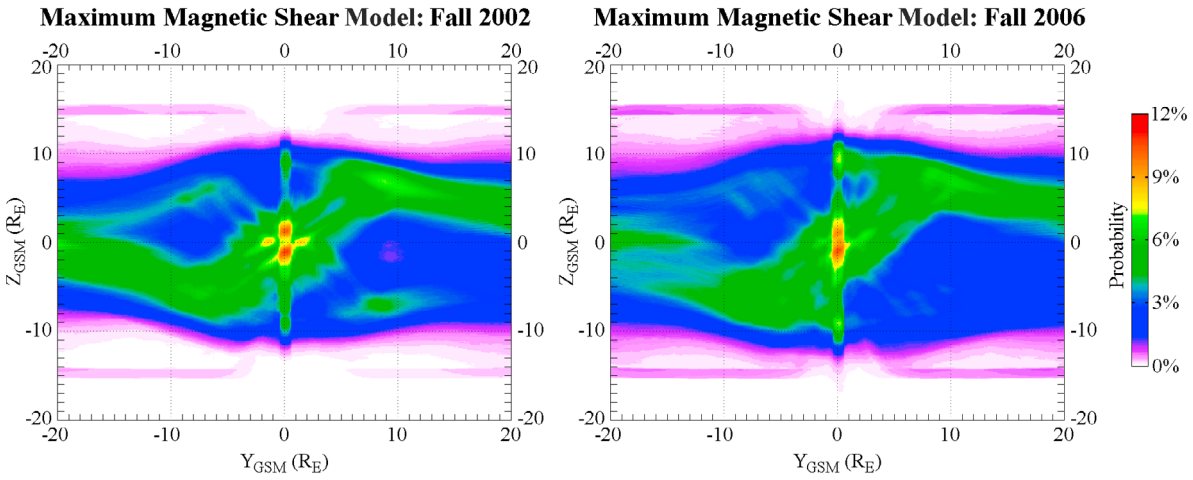

Figure 5. Comparison of reconnection line probability distributions (left) at solar maximum and (right) near solar minimum using the maximum magnetic shear model.

Figure 5 are due to the distribution of IMF conditions during a limited time period. Longer time periods would result in a smoothing-out of the striations.

4. Discussion and Conclusions

[22] A combined analytic and semiempirical model approach with solar wind observations as input has been used to investigate in a statistical manner the reconnection diffusion-region location probability across the dayside magnetopause. This method allows investigation of the likely locations of reconnection, as a function of Earth's seasonal dipole tilt and solar cycle. The x line model used is a maximum magnetic shear x line model that is contiguous along the magnetopause surface. This particular model has been developed from mappings by the polar TIMAS plasma distribution velocity cutoffs to the reconnection site and has been tested in a limited fashion with THEMIS magnetopause crossings. The models have been used to produce probability maps for the reconnection x line over the dayside magnetopause surface and how the probability varies as a function of month or season. It is found that, assuming an effective diffusion-region length of 1 R_E, the probability is maximal in the flank regions and is also a bit higher in localized regions near local noon. The maps also reveal that these patterns change very little from year to year, such that a link between solar cycle variability and probabilistic reconnection x line location is weak at best.

[23] This study represents the current best method for investigating reconnection x line locations using presently available models. Improved magnetic draping models [e.g., *Romashets et al.*, 2008] and magnetopause models may increase the result accuracy. Also, new data from NASA's MMS mission (currently in development) and other spacecraft will provide a more comprehensive understanding of the fundamental processes leading to reconnection and a refinement of current reconnection x line models.

[24] As one application, optimizing the orbital path chosen for the dayside magnetopause part of the MMS mission has been studied. Predicted magnetopause crossings for the MMS project baseline orbit (launch August 2014) are combined with a diffusion-region location probability map created using the maximum magnetic shear model and representative solar wind conditions from 2004 (i.e., from the same part of the solar cycle). The results are shown in Figure 6.

[25] The dayside orbit was chosen so that the satellite cluster would make several passes through the subsolar point, where traditional component reconnection models predict near-continuous reconnection. However, as has been shown, the high-probability reconnection region shifts northward or southward owing to the Earth's magnetic dipole tilt. Knowing only this a priori, one would expect that orbital parameters chosen to maximize the number of magnetopause crossings at the subsolar point to be nonoptimal. However, the current model MMS dayside-phase orbit is nearly optimal because the predicted magnetopause crossings track well the high-probability regions east and

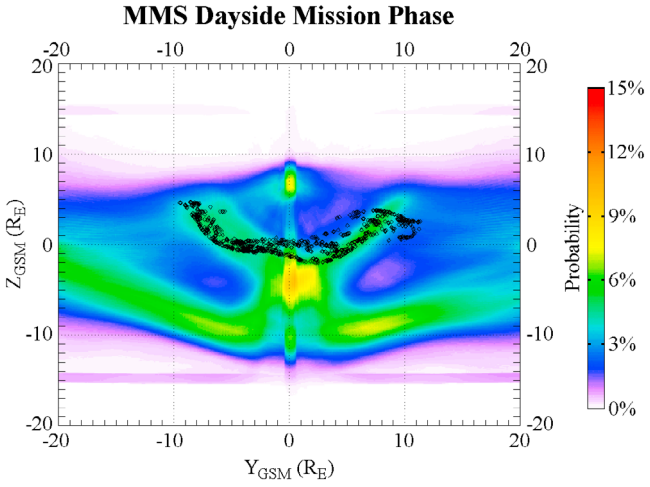

Figure 6. Projected MMS dayside magnetopause crossings overlain with a reconnection probability map spanning the time interval of the MMS dayside mission phase: May to August 2015 (using ACE observations from May to August 2004).

west of the noon meridian. While the methods used in this paper are coarse, they are useful for mission planning.

[26] **Acknowledgments.** The authors thank the ACE plasma (D. J. McComas) and magnetometer (E. J. Smith) teams for providing data via the NASA CDA Web site. The authors also thank the THEMIS team for providing magnetic field and plasma observations. This work was supported by NASA contracts NNX08AF35G and NNG05GE15G, and subcontract 499935Q (via SwRI) for MMS science. Masaki Fujimoto thanks the reviewers for their assistance in evaluating the manuscript.

[27] Masaki Fujimoto thanks the reviewers for their assistance in evaluating this paper.

References

Chandler, M. O., S. A. Fuselier, M. Lockwood, and T. E. Moore (1999), Evidence of component merging equatorward of the cusp, *Geophys. Res. Lett.*, *104*, 22,623–22,633.

Cooling, B. M. A., C. J. Owen, and S. J. Schwartz (2001), Role of the magnetosheath flow in determining the motion of open flux tubes, *J. Geophys. Res.*, *106*, 18,763–18,775.

Cowley, S. W. H. (1976), Comments on the merging of nonantiparallel magnetic fields, *J. Geophys. Res.*, *81*, 3455–3458.

Daughton, W., J. Scudder, and H. Karimabadi (2006), Fully kinetic simulations of undriven magnetic reconnection with open boundary conditions, *Phys. Plasmas*, *13*, 072101, doi:10.1063/1.2218817.

Drake, J. F., M. Swisdak, C. Cattell, M. A. Shay, B. N. Rogers, and A. Zeiler (2003), Formation of electron holes and particle energization during magnetic reconnection, *Science*, *299*, 873–877.

Dunlop, M., Q.-H. Zhang, C.-J. Xiao, J.-S. He, Z. Pu, R. C. Fear, C. Shen, and C. P. Escoubet (2009), Reconnection at high latitudes: Antiparallel merging, *Phys. Rev. Lett.*, *102*(7), 075005, doi:10.1103/PhysRevLett.102.075005.

Fuselier, S. A., K. J. Trattner, and S. M. Petrinec (2000), Cusp observations of high- and low-latitude reconnection for northward interplanetary magnetic field, *J. Geophys. Res.*, *105*, 253–266.

Fuselier, S. A., H. U. Frey, K. J. Trattner, S. B. Mende, and J. L. Burch (2002), Cusp aurora dependence on interplanetary magnetic field B_z, *J. Geophys. Res.*, *107*(A7), 1111, doi:10.1029/2001JA900165.

Gosling, J. T., M. F. Thomsen, S. J. Bame, and C. T. Russell (1986), Accelerated plasma flows at the near-tail magnetopause, *J. Geophys. Res.*, *91*, 3029–3041.

Hesse, M., K. Schindler, J. Birn, and M. Kuznetsova (1999), The diffusion region in collisionless magnetic reconnection, *Phys. Plasmas*, *6*, 1781–1795.

Hu, Y. Q., Z. Peng, C. Wang, and J. R. Kan (2009), Magnetic merging line and reconnection voltage versus IMF clock angle: Results from global MHD simulations, *J. Geophys. Res.*, *114*, A08220, doi:10.1029/2009JA014118.

Karimabadi, H., W. Daughton, and J. Scudder (2007), Multi-scale structure of the electron diffusion region, *Geophys. Res. Lett.*, *34*, L13104, doi:10.1029/2007GL030306.

Kobel, E., and E. O. Flückiger (1994), A model of the steady state magnetic field in the magnetosheath, *J. Geophys. Res.*, *99*, 23,617–23,622.

Lau, Y. T., and J. M. Finn (1990), Three-dimensional kinematic reconnection in the presence of field nulls and closed field lines, *Astrophys. J.*, *350*, 672–691.

Luhmann, J. G., T.-L. Zhang, S. M. Petrinec, C. T. Russell, P. Gazis, and A. Barnes (1993), Solar cycle 21 effects on the interplanetary magnetic field and related parameters at 0.7 and 1.0 AU, *J. Geophys. Res.*, *98*, 5559–5572.

McComas, D. J., S. J. Bame, P. Barker, W. C. Feldman, J. L. Phillips, P. Riley, and J. W. Griffee (1998), Solar Wind Electron Proton Alpha Monitor (SWEPAM) for the Advanced Composition Explorer, *Space Sci. Rev.*, *86*, 563–612.

Moore, T. E., M.-C. Fok, and M. O. Chandler (2002), The dayside reconnection x line, *J. Geophys. Res.*, *107*(A10), 1332, doi:10.1029/2002JA009381.

Mozer, F. S., S. D. Bale, and T. D. Phan (2002), Evidence of diffusion regions at a subsolar magnetopause crossing, *Phys. Rev. Lett.*, *89*, 015002, doi:10.1103/PhysRevLett.89.015002.

Mozer, F. S., V. Angelopoulos, J. Bonnell, K. H. Glassmeier, and J. P. McFadden (2008), THEMIS observations of modified Hall fields in asymmetric magnetic field reconnection, *Geophys. Res. Lett.*, *35*, L17S04, doi:10.1029/2007GL033033.

Onsager, T. G., M. F. Thomsen, J. T. Gosling, and S. J. Bame (1990), Electron distributions in the plasma sheet boundary layer: Time-of-flight effects, *Geophys. Res. Lett.*, *17*, 1837–1840.

Park, K. S., T. Ogino, and R. J. Walker (2006), On the importance of antiparallel reconnection when the dipole tilt and IMF B_y are nonzero, *J. Geophys. Res.*, *111*, A05202, doi:10.1029/2004JA010972.

Paschmann, G., N. Sckopke, S. J. Bame, J. R. Asbridge, J. T. Gosling, C. T. Russell, and E. W. Greenstadt (1979), Plasma acceleration at the Earth's magnetopause: Evidence for reconnection, *Nature*, *282*, 243–246.

Phan, T. D., et al. (2000), Extended magnetic reconnection at the Earth's magnetopause from detection of bi-directional jets, *Nature*, *404*, 848–850.

Phan, T. D., H. Hasegawa, M. Fujimoto, M. Øieroset, T. Mukai, R. P. Lin, and W. Paterson (2006), Simultaneous Geotail and Wind observations of reconnection at the subsolar and tail flank magnetopause, *Geophys. Res. Lett.*, *33*, L09104, doi:10.1029/2006GL025756.

Phan, T. D., J. F. Drake, M. A. Shay, F. S. Mozer, and J. P. Eastwood (2007), Evidence for an elongated (>60 ion skin depths) electron diffusion region during fast magnetic reconnection, *Phys. Rev. Lett.*, *99*, 255002, doi:10.1103/99.255002.

Pritchett, P. L., and F. S. Mozer (2009), Asymmetric magnetic reconnection in the presence of a guide field, *J. Geophys. Res.*, *114*, A11210, doi:10.1029/2009JA014343.

Pu, Z. Y., et al. (2007), Global view of dayside magnetic reconnection with the dusk-dawn IMF orientation: A statistical study for Double Star and Cluster data, *Geophys. Res. Lett.*, *34*, L20101, doi:10.1029/2007GL030336.

Romashets, E. P., S. Poedts, and M. Vandas (2008), Modeling the magnetic field in the magnetosheath region, *J. Geophys. Res.*, *113*, A02203, doi:10.1029/2006JA012072.

Russell, C. T., and R. L. McPherron (1973), Semiannual variation of geomagnetic activity, *J. Geophys. Res.*, *78*, 92–108.

Scudder, J. D., F. S. Mozer, N. C. Maynard, and C. T. Russell (2002), Fingerprints of collisionless reconnection at the separator: 1. Ambipolar-Hall signatures, *J. Geophys. Res.*, *107*(A10), 1294, doi:10.1029/2001JA000126.

Shay, M. A., J. F. Drake, and M. Swisdak (2007), Two-scale structure of the electron dissipation region during collisionless magnetic reconnection, *Phys. Rev. Lett.*, *99*, 155002, doi:10.1103/PhysRevLett.99.155002.

Smith, C. W., M. H. Acuna, L. F. Burlaga, J. L'Heureux, N. F. Ness, and J. Scheifele (1998), The ACE Magnetic Field Experiment, *Space Sci. Rev.*, *86*, 613–632.

Song, P., R. C. Elphic, and C. T. Russell (1988), ISEE 1 and 2 observations of the oscillating magnetopause, *Geophys. Res. Lett.*, *15*, 744–747, doi:10.1029/GL015i008p00744.

Sonnerup, B. U. Ö. (1974), The reconnecting magnetosphere, in *Magnetospheric Physics*, *Proceedings of the Advanced Summer Institute*, *Held at Sheffield, UK, 1973*, vol. 44, edited by B. M. McCormas, p. 23, Reidel, Dordrecht, Neth.

Sonnerup, B. U. Ö., G. Paschmann, I. Papamastorakis, N. Sckopke, G. Haerendel, S. J. Bame, J. R. Asbridge, J. T. Gosling, and C. T. Russell (1981), Evidence for reconnection at the Earth's magnetopause, *J. Geophys. Res.*, *86*, 10,049–10,067.

Trattner, K. J., J. S. Mulcock, S. M. Petrinec, and S. A. Fuselier (2007), Probing the boundary between antiparallel and component reconnection during southward interplanetary magnetic field conditions, *J. Geophys. Res.*, *112*, A08210, doi:10.1029/2007JA012270.

Tsyganenko, N. (1995), Modeling the Earth's magnetospheric magnetic field confined within a realistic magnetopause, *J. Geophys. Res.*, *100*, 5599–5612.

Wang, X. G., and A. Bhattacharjee (1996), A three-dimensional reconnection model of the magnetosphere: Geometry and kinematics, *J. Geophys. Res.*, *101*, 2641–2653, doi:10.1029/95JA02184.

V. Angelopoulos, Institute of Geophysics and Planetary Physics, University of California, Los Angeles, CA 90065, USA.

J. L. Burch, Southwest Research Institute, San Antonio, TX 78228, USA.

S. A. Fuselier, S. M. Petrinec, and K. J. Trattner, Lockheed Martin Advanced Technology Center, Palo Alto, CA 94304, USA. (petrinec@spasci.com)

S. T. Griffiths, Department of Physics and Astronomy, University of Iowa, Iowa City, IA 52242, USA.

T. D. Phan, Space Sciences Laboratory, University of California, Berkeley, CA 94720, USA.